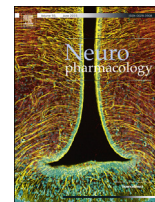




Contents lists available at ScienceDirect

Neuropharmacology

journal homepage: www.elsevier.com/locate/neuropharm

Neuroigin 2 deletion alters inhibitory synapse function and anxiety-associated neuronal activation in the amygdala

Olga Babaev^a, Paolo Botta^b, Elisabeth Meyer^b, Christian Müller^b,
Hannelore Ehrenreich^c, Nils Brose^a, Andreas Lüthi^b, Dilja Krueger-Burg^{a,*}

^a Department of Molecular Neurobiology, Max Planck Institute of Experimental Medicine, Hermann-Rein-Str. 3, 37075 Göttingen, Germany

^b Friedrich Miescher Institute for Biomedical Research, Maulbeerstr. 66, 4058 Basel, Switzerland

^c Clinical Neuroscience, Max Planck Institute of Experimental Medicine, Hermann-Rein-Str. 3, 37075 Göttingen, Germany

ARTICLE INFO

Article history:

Received 26 April 2015

Received in revised form

20 June 2015

Accepted 25 June 2015

Available online xxx

Keywords:

Neuroigins

Amygdala

Anxiety

Gephyrin

Inhibitory synapse

cFos

ABSTRACT

Neuroigin 2 (Nlgn2) is a synaptic adhesion protein that plays a central role in the maturation and function of inhibitory synapses. Nlgn2 mutations have been associated with psychiatric disorders such as schizophrenia, and in mice, deletion of Nlgn2 results in a pronounced anxiety phenotype. To date, however, the molecular and cellular mechanisms linking Nlgn2 deletion to psychiatric phenotypes remain completely unknown. The aim of this study was therefore to define the role of Nlgn2 in anxiety-related neural circuits. To this end, we used a combination of behavioral, immunohistochemical, and electrophysiological approaches in Nlgn2 knockout (KO) mice to expand the behavioral characterization of these mice and to assess the functional consequences of Nlgn2 deletion in the amygdala. Moreover, we investigated the differential activation of anxiety-related circuits in Nlgn2 KO mice using a cFOS activation assay following exposure to an anxiogenic stimulus. We found that Nlgn2 is present at the majority of inhibitory synapses in the basal amygdala, where its deletion affects postsynaptic structures specifically at perisomatic sites and leads to impaired inhibitory synaptic transmission. Following exposure to an anxiogenic environment, Nlgn2 KO mice show a robust anxiety phenotype as well as exacerbated induction of cFOS expression specifically in CaMKII-positive projection neurons, but not in parvalbumin- or somatostatin-positive interneurons. Our data indicate that Nlgn2 deletion predominantly affects inhibitory synapses onto projection neurons in basal amygdala, resulting in decreased inhibitory drive onto these neurons and leading to their excessive activation under anxiogenic conditions.

© 2015 Published by Elsevier Ltd.

1. Introduction

A major challenge in biological psychiatry lies in the vast heterogeneity of genetic and environmental factors that contribute to the etiology of most psychiatric disorders. Accordingly, research efforts are increasingly focusing on the identification of shared pathophysiological mechanisms that may present viable targets for the development of novel treatment strategies. In recent years, the notion that one such common mechanism may be dysregulation of synaptic function has gained considerable interest (Luthi and Luscher, 2014; Sudhof, 2008). A plethora of mutations in synaptic proteins has been associated with disorders such as autism and

schizophrenia, and significant efforts are currently underway to enhance our understanding of the link between perturbations in synaptic proteins and mental illness.

One family of synaptic proteins that has been prominently linked to psychiatric disorders are the Neuroigins (Nlgns) (Sudhof, 2008). Nlgns are postsynaptic adhesion proteins that modulate synapse maturation and function through transsynaptic interactions with Neurexins and through postsynaptic interactions with receptors and scaffolding proteins (Craig and Kang, 2007; Krueger et al., 2012). Neuroigin 2 (Nlgn2), whose loss of function was recently associated with schizophrenia (Sun et al., 2011), is thought to be expressed exclusively at inhibitory synapses (Graf et al., 2004; Varoqueaux et al., 2004) and to mediate anchoring of GABA_A receptors to the postsynaptic membrane via interactions with collybistin and gephyrin (Pouloupoulos et al., 2009; Soykan et al., 2014). Deletion of Nlgn2 leads to alterations in the

* Corresponding author.

E-mail address: krueger@em.mpg.de (D. Krueger-Burg).

molecular composition of inhibitory synapses, e.g. of perisomatic synapses in the stratum pyramidale in hippocampus and the dentate gyrus granule cell layer, and to perturbations of inhibitory synaptic transmission, e.g. in brainstem, somatosensory cortex, and hippocampus, emphasizing its essential role in the maintenance of excitation/inhibition (E/I) balance in the brain (Gibson et al., 2009; Jedlicka et al., 2011; Pouloupoulos et al., 2009).

Surprisingly, in view of the widespread expression of Nlgn2 throughout the brain, Nlgn2 knockout (KO) mice display relatively selective deficits in behavior domains related to anxiety (Blundell et al., 2009), rather than global behavioral impairments that might be expected from a general alteration in E/I balance. This observation is particularly interesting in light of recent research showing that the precise role of Nlgn2 is highly dependent on synaptic context (Foldy et al., 2013; Rothwell et al., 2014), highlighting the fundamental importance of studying these molecules *in vivo* in the context of specific intact circuits and behaviors. The prominent anxiety phenotype in Nlgn2 KO mice indicates that Nlgn2 must play a central role in the neural circuitry underlying anxiety behaviors, but to date, virtually nothing is known about the function of Nlgn2 in these circuits. To address this problem, we investigated the molecular, cellular and physiological consequences of Nlgn2 KO in the amygdala, a brain region that has been prominently implicated in fear and anxiety behaviors (Luthi and Luscher, 2014).

2. Materials and methods

2.1. Experimental animals

Nlgn2 KO mice (Varoqueaux et al., 2006) were generated in our laboratory on a 129/Sv background and were backcrossed onto a C57BL/6J background for at least six generations. Male wildtype (WT), heterozygous (Het) and homozygous (KO) littermates were obtained from Nlgn2 heterozygous breeding pairs (behavioral and immunohistochemical experiments) or from Nlgn2 homozygous breeding pairs and age-matched wild-type C57BL/6J controls (Harlan Ltd, electrophysiological experiments). All mice were 2–3 months old at the beginning of the experiment. Animals were maintained on a 12 h light/dark cycle, with food and water *ad libitum*. All experiments were performed during the light cycle (with the exception of home cage activity monitoring as described below). The experimenter was blind to genotype during all stages of data acquisition and analysis. All procedures were carried out in agreement with the guidelines for the welfare of experimental animals issued by the Federal Government of Germany and the Max Planck Society (anxiety and locomotor testing, immunohistochemistry) or the Veterinary Department of the Canton of Basel-Stadt (electrophysiology).

2.2. Behavioral characterization

Additional information on experimental procedures is provided in Supplement 1.

2.2.1. Assessment of anxiety

To assess anxiety levels, animals were subjected to the following three anxiety tests on consecutive days: Elevated plus maze (EPM), open field test (OFT), and light/dark test (LDT) (Table S1 in Supplement 1). Performance was recorded using an overhead camera system and scored automatically using the Viewer software (Biobserve, St. Augustin, Germany).

2.2.2. Assessment of home cage activity

Recording of home cage activity was performed using the

LABORAS system and software (Metris, Hoofddorp, The Netherlands). The following aspects of activity were recorded: total distance travelled and duration of locomotion, immobility, climbing, grooming and circling (Table S2 in Supplement 1).

2.2.3. Assessment of freezing in a novel environment

Mice were placed inside a fear conditioning chamber (25 × 30 cm; Med Associates, St. Albans, VT, USA) with a camera fixed on one of the internal walls. Freezing behavior was recorded for a period of 2 min and scored automatically using the Video Freeze software (Med Associates, St. Albans, VT, USA) with the motion detection threshold set to 60.

2.3. Immunohistochemistry procedures

2.3.1. Immunolabeling for presynaptic markers

For VIAAT immunolabeling, animals were perfused transcardially with 4% PFA in 0.1 M phosphate buffer (PB), brains were post-fixed in PFA overnight, and cryoprotected in 30% sucrose in 0.1 M PB. Free floating sections, prepared using a Leica CM3050S cryostat (Leica, Wetzlar, Germany), were incubated in blocking solution for 1 h, and then labeled with primary and secondary antibodies as detailed in Table S3 (Supplement 1). Sections were washed with phosphate-buffered saline (PBS) after each incubation, and were finally mounted on glass slides using Aqua-Poly/Mount (Polysciences, Eppelheim, Germany).

2.3.2. Immunolabeling for postsynaptic markers

Immunolabeling for PSD-95, gephyrin, and Nlgn2 was performed on methanol-fixed fresh frozen brain sections using a modified version of a published protocol (11). Briefly, the brains were frozen immediately after dissection in an isopentane bath at –35 °C to –40 °C. Coronal sections were prepared using a Leica CM3050S cryostat (Leica, Wetzlar, Germany), mounted on glass slides, and dried at room temperature. Sections were then fixed in methanol at –20 °C for 5 min, blocked for 1 h, and labeled with primary and secondary antibodies as detailed in Table S3 (Supplement 1). Sections were washed with PBS after each incubation. The slides were then dried overnight at 4 °C, and covered with mounting media (Aqua-Poly/Mount; Polysciences, Eppelheim, Germany) and glass coverslips.

2.3.3. cFOS assay and characterization of cFOS activation pattern

To assess anxiety-induced cFOS activation, mice were first exposed to the open field chamber for 10 min, and were then sacrificed and perfused 90 min after exposure. Perfused brains were processed as described above for VIAAT immunolabeling. A detailed description of the histochemical procedures is provided in Table S3 (Supplement 1). Washing steps and mounting were performed as described above.

2.4. Image acquisition, electrophysiology, and data analysis

Images were acquired using a confocal laser scanning microscope (Leica SP2; Leica, Wetzlar, Germany). For each WT-KO pair, sections were anatomically matched and the settings for laser power, gain, and offset were kept constant during imaging. Detailed descriptions of acquisition parameters and analysis methods are given in Table S4 (Supplement 1).

2.4.1. Imaging of synaptic markers

Images of synaptic markers (gephyrin, PSD-95, Nlgn2, and VIAAT) were obtained using a 63× oil immersion objective. The number and size of particles, as well as mean fluorescence intensity, were quantified in the area surrounding the cell body, and

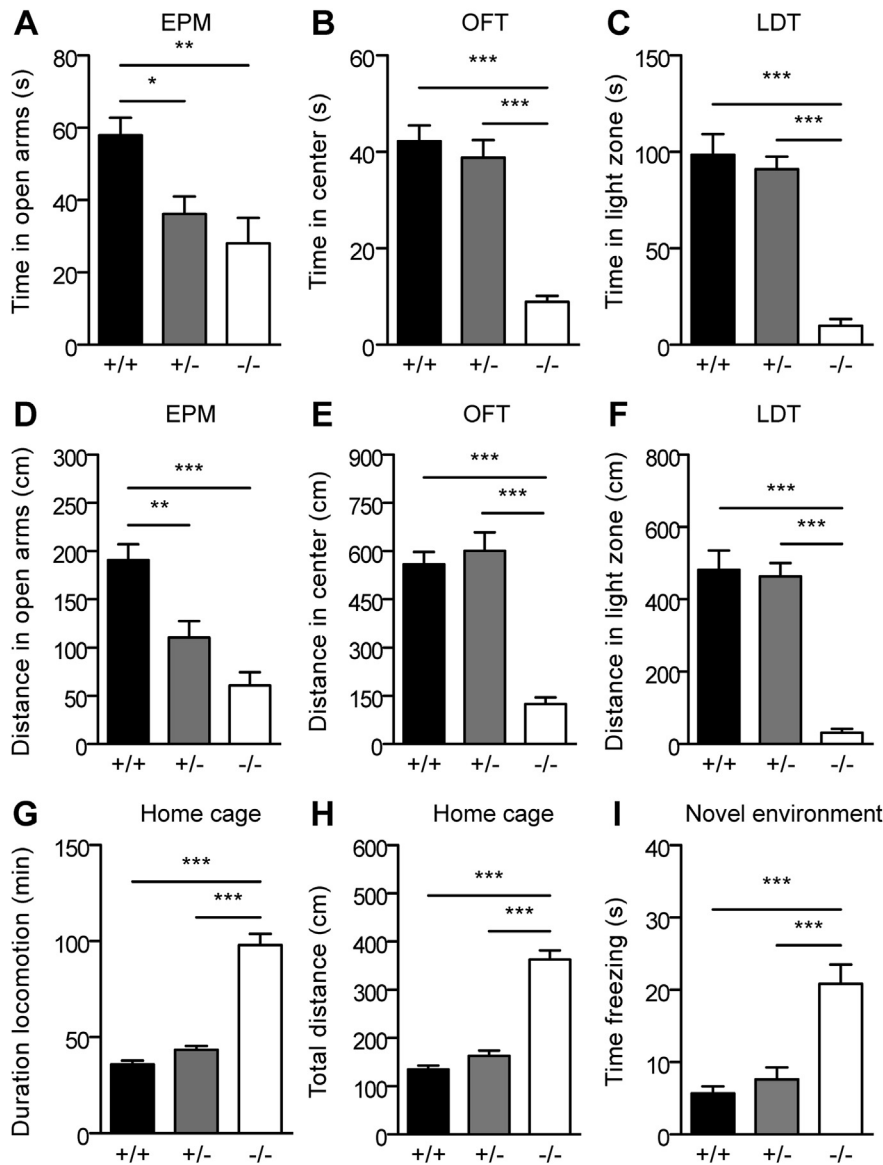


Fig. 1. Anxiety phenotype and locomotor activity of Nlgn2 KO mice. (A–C) Time spent by WT, Nlgn2 Het, and Nlgn2 KO mice in the open arms of elevated plus maze (A), center of the open field (B), and light zone of light dark box (C). One-way ANOVA for genotype: (A) $F_{2,43} = 7.07$, $p < 0.01$; (B) $F_{2,43} = 37.33$, $p < 0.0001$; (C) $F_{2,44} = 42.73$, $p < 0.0001$. (D–F) Distance traveled in the open arms of elevated plus maze (D), center of the open field (E), and light zone of light dark box (F). One-way ANOVA for genotype: (D) $F_{2,43} = 15.83$, $p < 0.0001$; (E) $F_{2,44} = 35.43$, $p < 0.0001$; (F) $F_{2,45} = 44.62$, $p < 0.0001$. (G, H) Duration of locomotor activity (G) and distance traveled (H) in a home cage setting during 15 h of recording. One-way ANOVA for genotype: (G) $F_{2,43} = 79.75$, $p < 0.0001$; (H) $F_{2,46} = 61.95$, $p < 0.0001$. (I) Duration of freezing in a novel environment. One-way ANOVA for genotype: (I) $F_{2,44} = 17.98$, $p < 0.0001$. Post hoc Tukey's test: * $p < 0.05$, ** $p < 0.01$, *** $p < 0.001$. $n = 14–18$ for each genotype. All bars represent mean + SEM.

the number of particles per area was divided by the length of the cell body perimeter to obtain the final result. Colocalization of synaptic markers was analyzed using Imaris software (Bitplane, Zurich, Switzerland).

2.4.2. Imaging of cFOS and cellular markers

Images of cFOS and cellular markers were obtained using a 40 \times oil immersion objective as described in Table S4 (Supplement 1). cFOS images were thresholded manually in ImageJ with the same threshold value for WT and Nlgn2 KO in each pair, and single- and double-labeled cells were then quantified using Imaris (Bitplane, Zurich, Switzerland).

2.5. Slice electrophysiology

Standard procedures were used to prepare 300 μ M thick coronal slices. The brain was dissected in ice-cold artificial cerebrospinal fluid (ACSF), mounted on an agar block, and sliced with a vibrating-blade microtome (HM 650 V; Carl Zeiss, Jena, Germany) at 4 $^{\circ}$ C. Slices were maintained for 45 min at 37 $^{\circ}$ C in an interface chamber containing ACSF equilibrated with 95% O₂/5% CO₂ (Table S5 in Supplement 1). Recordings were performed with ACSF in a recording chamber at a temperature of 35 $^{\circ}$ C and at a perfusion rate of 1–2 ml/min. Neurons were visually identified with infrared video microscopy using an upright microscope equipped with a 40X objective (Olympus, Tokyo, Japan). Patch electrodes (3–5 M Ω)

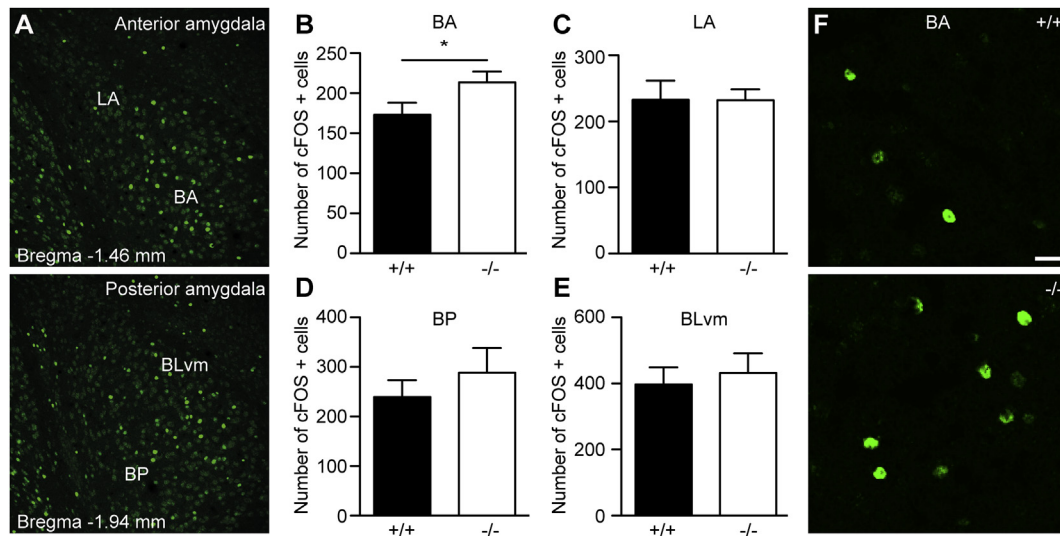


Fig. 2. Anxiety-induced cFOS expression in basolateral amygdala of Nlgn2 KO mice. (A) Low magnification photomicrographs of cFOS labeled basolateral amygdala indicate the regions included in the analysis. Scale bar, 100 μ m. (B–E) Quantification of cFOS positive cells in anterior BA (B), lateral amygdala (C), posterior BA (D), and basolateral ventromedial amygdala (E) in WT and Nlgn2 KO mice. cFOS expression was triggered by exposure to novel environment. (F) Representative photomicrographs of cFOS expression in anterior BA of WT and Nlgn2 KO mice after exposure to novel environment. Scale bar, 20 μ m. Paired Student's t-test: * $p < 0.05$. $n = 6$ for each genotype in figures B, D and E, $n = 5$ for each genotype in figure C. All bars represent mean + SEM.

were pulled from borosilicate glass tubing. For voltage clamp experiments to record miniature inhibitory post-synaptic currents (mIPSCs), patch electrodes were filled with an internal solution (Table S5 in Supplement 1). Whole cell patch-clamp recordings were excluded if the access resistance exceeded 13 M Ω and/or changed more than 20% during the recordings. Data were recorded with a MultiClamp 700B amplifier (Molecular Devices, Sunnyvale, CA, USA), filtered at 0.2 kHz, and digitized at 10 kHz. Data were acquired and analyzed with Clampex 10.0, Clampfit 10.0 (Molecular Devices, Sunnyvale, CA, USA) and the Mini Analysis Program (Synaptosoft, Decatur, GA).

2.6. Statistical analyses

All data were analyzed statistically using Prism (GraphPad Software, La Jolla, CA, USA). Outliers, defined as data points that were two standard deviations above or below the mean, were removed prior to statistical analysis and were excluded from the graphical representation in the figures (relevant for Figs. 1 and 2C, S1 and S2). Behavioral scores were subjected to one-way ANOVA or two-way ANOVA, and post-hoc Tukey's tests were used for comparison between groups. Data obtained from histological experiments were analyzed using paired, two tailed Student's t-tests. Data obtained from electrophysiological experiments were analyzed using unpaired, two tailed Student's t-tests.

3. Results

3.1. Nlgn2 KO causes a robust anxiety phenotype

Nlgn2 KO mice have previously been reported to display increased anxiety-related behaviors (Blundell et al., 2009), but the extent of this anxiety phenotype has been discussed controversially (Blundell et al., 2009; Wohr et al., 2013). To address this issue and to characterize the anxiety phenotype under our experimental conditions, we performed a battery of anxiety tests on Nlgn2 KO, Nlgn2 Het and WT littermates, including the elevated plus maze (EPM), the open field test (OFT) and the light/dark exploration test (LDT). Nlgn2 KO mice showed a robust anxiety phenotype in all of these

tests (Fig. 1; Fig. S1 in Supplement 1), spending significantly less time and making fewer entries into the open arms of the EPM, the center of the OFT, and the light zone of the LDT (Fig. 1A–C; Fig. S1A in Supplement 1). Similarly, the distance traveled in the open arms of the EPM, the center of the OFT, and the light zone of the LDT was significantly reduced in Nlgn2 KO mice (Fig. 1D–F). Nlgn2 Het mice exhibited a mild anxiety phenotype only in the EPM (Fig. 1A,D; Fig. S1A in Supplement 1), with no significant differences from WT mice observed in the other two anxiety tests (Fig. 1B,C,E,F; Fig. S1 in Supplement 1). Given that Nlgn2 Het mice showed only a very mild behavioral phenotype, the subsequent molecular, cellular, and electrophysiological characterization was restricted to the comparison of WT and Nlgn2 KO mice.

3.2. Nlgn2 KO causes reduced locomotor activity and enhanced freezing specifically under anxiogenic conditions

Interestingly, the total distance traveled by Nlgn2 KO mice in the EPM and OFT was also significantly reduced as compared to WT and Het mice (Fig. S1B,C in Supplement 1; this analysis could not be performed for the LDT for technical reasons, since our experimental setup did not permit us to measure activity levels in the dark zone). To determine whether this reduction in locomotor activity may confound the anxiety phenotype in the KO mice, we performed three additional analyses. First, we normalized the distance traveled in the open arms of the EPM and the center of the OFT to the total distance traveled in the EPM and OFT, respectively (Fig. S1D,E in Supplement 1). This analysis revealed that the anxiety phenotype is still highly significant even after correcting for overall activity levels. Second, to rule out a primary locomotor impairment, we monitored activity under basal, non-anxiogenic conditions in a home cage setting. Under these conditions, Nlgn2 KO mice surprisingly showed an increase in locomotion (Fig. 1G,H) and a corresponding decrease in time spent immobile (Fig. S2A in Supplement 1), while additional aspects of home cage activity did not differ (Fig. S2B–D in Supplement 1). Third, based on the empirical observation that Nlgn2 KO mice showed increased freezing during the anxiety tests, we also directly measured freezing behavior in a novel anxiogenic environment. Nlgn2 KO

mice spent significantly more time freezing following first exposure to a novel chamber (Fig. 11). This increase in freezing likely contributes to the reduced exploratory activity, which is therefore one of the manifestations of the robust anxiety phenotype in Nlgn2 KO mice.

3.3. Enhanced cFOS activation in basal amygdala neurons of Nlgn2 KO mice upon exposure to an anxiogenic environment

To elucidate the cellular and molecular basis for the anxiety phenotype in Nlgn2 KO mice, we investigated whether differential activation of neurons could be observed in various brain regions associated with anxiety processing, including the amygdala and prefrontal cortex (Luthi and Luscher, 2014; Singewald et al., 2003). To this end, we exposed WT and Nlgn2 KO mice to an anxiogenic environment (10 min in an open field arena) and subsequently used an immunohistochemical approach to assess the expression of cFOS, a marker of neuronal activity (Sagar et al., 1988). In the amygdala (Fig. 2A), we observed an increase in overall cFOS activation of basal amygdala (BA) neurons in Nlgn2 KO mice, which was significant in the anterior basal region (Fig. 2B; $p < 0.05$), but not in lateral, posterior, or ventromedial regions (Fig. 2C–E). This increase was triggered by the anxiogenic situation, since cFOS expression under basal conditions did not significantly differ between WT and Nlgn2 KO mice (Fig. S3A–B in Supplement 1). In contrast, we observed no genotype difference in cFOS immunoreactivity in two areas of prefrontal cortex, the infralimbic (Fig. S4A in Supplement 1) and prelimbic cortices (Fig. S4B in Supplement 1). These findings indicate that the BA is one of the brain regions involved in the anxiety phenotype of Nlgn2 KO mice, and we therefore focused our further analyses on this region.

3.4. Nlgn2 is localized to inhibitory synapses in the basal amygdala

To investigate the molecular mechanisms underlying the increased anxiety-triggered activation of BA neurons in Nlgn2 KOs, we first assessed the expression pattern of Nlgn2 in the amygdala of WT mice. We found that Nlgn2 is highly expressed in the basal nucleus but not in the central nucleus of the amygdala (Fig. 3A). To characterize which synapses contain Nlgn2 in this region, we performed double labeling of Nlgn2 with PSD-95, a marker of excitatory synapses, and with gephyrin, a marker of inhibitory synapses. Our data show that Nlgn2 colocalizes with gephyrin (Fig. 2B; Pearson's correlation coefficient = 0.62) but not with PSD-95 (Fig. 2C; Pearson's correlation coefficient = 0.01), consistent with previous reports on Nlgn2 distribution in other brain regions, including retina and hippocampus (Hoon et al., 2009; Pouloupoulos et al., 2009; Varoqueaux et al., 2004). Approximately 76% of Nlgn2 puncta were colocalized with gephyrin, indicating that Nlgn2 is

localized primarily to inhibitory synapses in BA. Interestingly, 78% of gephyrin puncta were also positive for Nlgn2, indicating that Nlgn2 is present at the majority of inhibitory synapses in BA.

3.5. Nlgn2 KO perturbs the composition of perisomatic postsynaptic sites in the basal amygdala

Given the localization pattern of Nlgn2 at inhibitory synapses, we next investigated whether the loss of Nlgn2 affects the structure of inhibitory synapses in the BA by quantifying the number and intensity of gephyrin puncta. The overall gephyrin intensity was not altered upon Nlgn2 loss (Fig. 4A–B). However, a specific analysis of perisomatic regions (Fig. 4C–D) revealed a significant reduction in the number, size, and intensity of gephyrin puncta in Nlgn2 KOs (Fig. 4E–G). To investigate whether this reduction is caused by a decrease in the total number of inhibitory synapses, we stained for the vesicular inhibitory amino acid transporter (VIAAT), a marker of inhibitory presynaptic terminals (Fig. 5A), and found that the number and size of perisomatic VIAAT puncta are not altered upon Nlgn2 deletion (Fig. 5B–C). To confirm this finding, we quantified the number of parvalbumin (PV) puncta in the BA (Fig. 5D). PV-positive interneurons are the major source of perisomatic synapses in BA (Muller et al., 2006; Spanpanato et al., 2011), and PV puncta therefore specifically represent perisomatic inhibitory presynaptic sites. The number and intensity of PV-positive puncta was not altered in Nlgn2 KO mice (Fig. 5E–F). Taken together, these findings imply that Nlgn2 deletion does not result in a decrease in overall inhibitory synapse number in BA, but instead primarily affects the molecular composition of perisomatic inhibitory postsynaptic sites.

3.6. Nlgn2 KO impairs inhibitory synaptic transmission in the basal amygdala

To assess whether deletion of Nlgn2 alters synaptic transmission, we measured miniature inhibitory postsynaptic currents (mIPSCs) in the BA and central amygdala (CeA, Fig. 6). A pronounced reduction in mIPSC frequency (Fig. 6E) but not amplitude (Fig. 6F) was observed in BA of Nlgn2 KO mice, while mIPSC kinetics were not significantly altered (rise time: WT = 1.40 ms, KO = 1.57 ms, $p = 0.13$; decay time: WT = 4.14 ms, KO = 2.87 ms, $p = 0.09$). In CEa, no changes were observed in mIPSC frequency (Fig. 6G) or amplitude (Fig. 6H).

3.7. Nlgn2 KO has differential effects on anxiety-associated activation of glutamatergic and GABAergic neurons in the basal amygdala

BA is a cortex-like structure that contains both glutamatergic

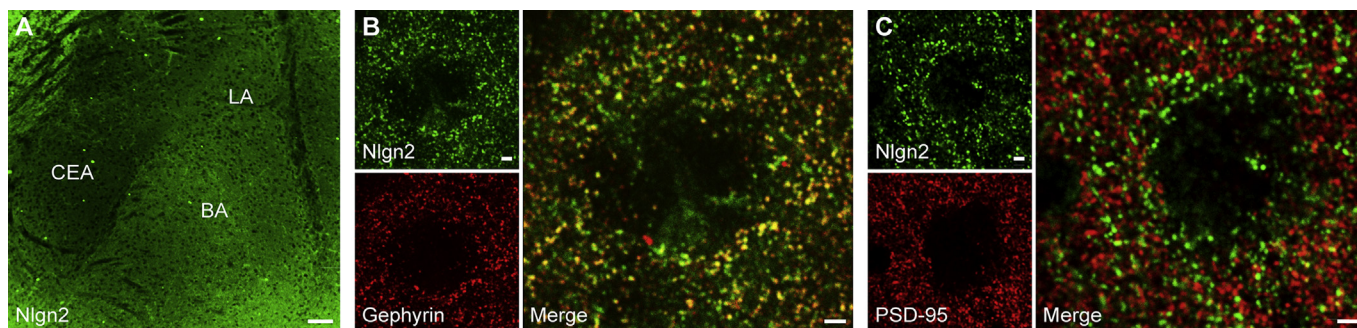


Fig. 3. Nlgn2 localization in the amygdala. (A) Immunostaining shows that Nlgn2 is highly expressed in the basal and lateral nuclei of the amygdala, with a lower level in CEA. Scale bar, 100 μm . (B, C) Colocalization of Nlgn2 with gephyrin, a marker of inhibitory synapses (B), and PSD-95, a marker of excitatory synapses (C). Scale bar, 2 μm .

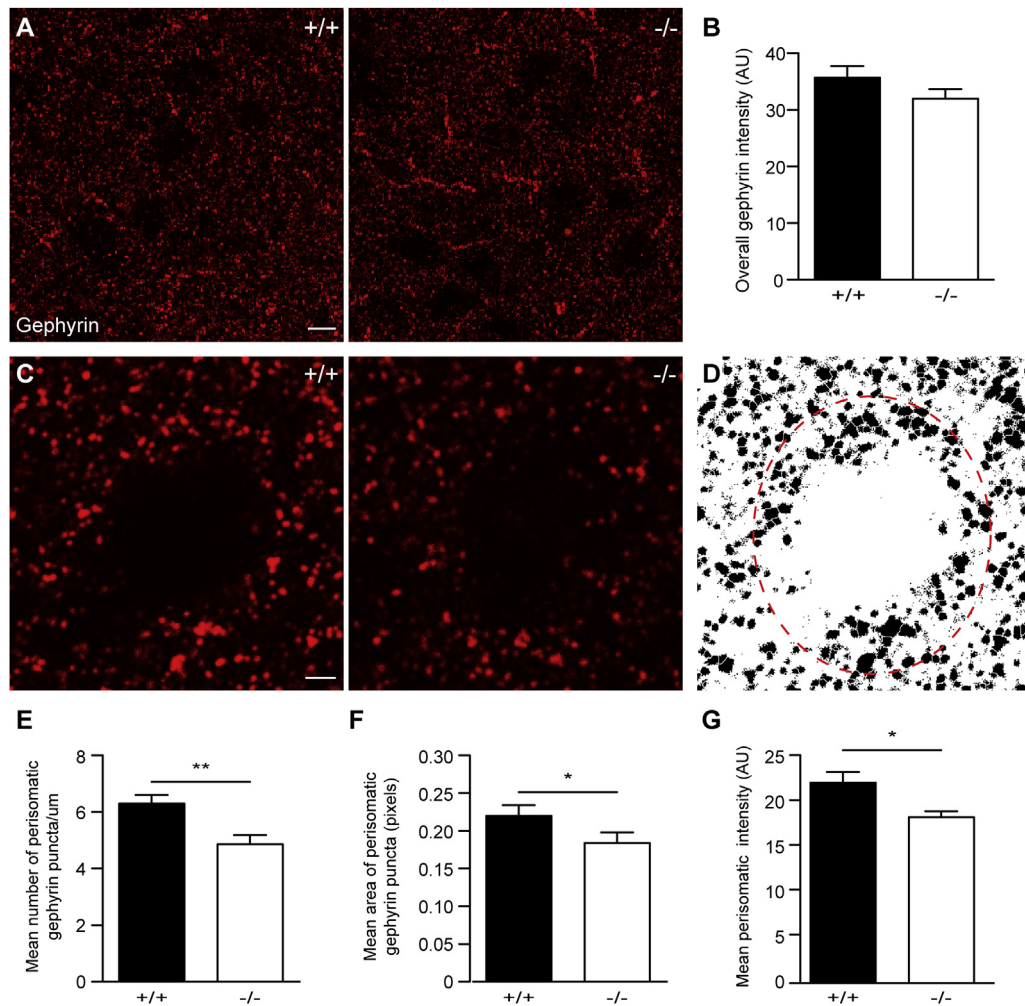


Fig. 4. Localization and expression levels of gephyrin in BA of Nlgn2 KO mice. (A) Photomicrographs show overall gephyrin distribution in BA of WT and Nlgn2 KO mice. Scale bar, 10 μ m. (B) Mean fluorescence intensity of overall gephyrin immunostaining. $n = 6$ for each genotype. (C, D) High magnification photomicrographs show perisomatic gephyrin localization in BA of WT and Nlgn2 KO (C). The perisomatic area is indicated on a thresholded image (D). Scale bar, 2 μ m. (E–G) Mean number per cell perimeter (E), mean area (F), and mean intensity (G) of perisomatic gephyrin puncta in BA. $n = 8$ for each genotype. Paired, two-tailed Student's *t*-test: * $p < 0.05$, ** $p < 0.01$. All bars represent mean + SEM.

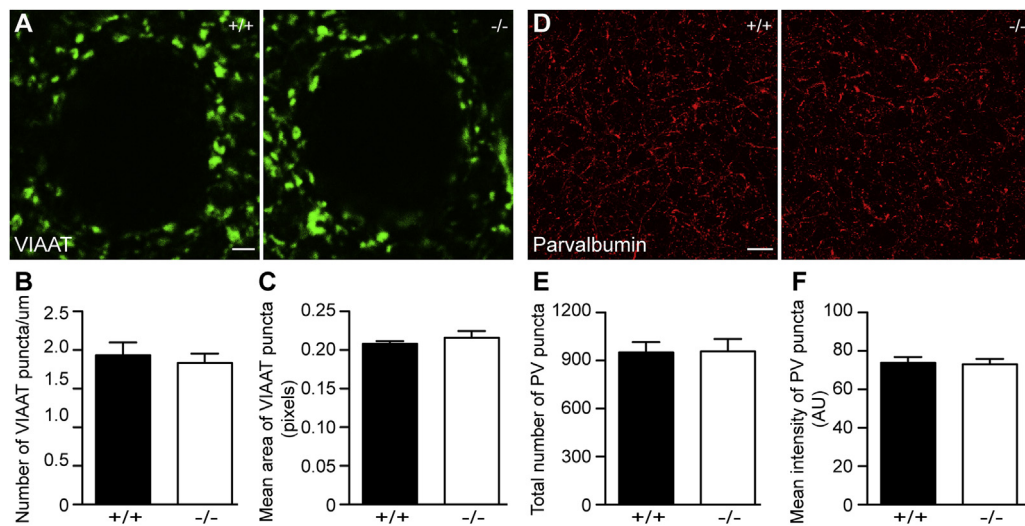


Fig. 5. Localization and expression levels of presynaptic inhibitory markers in BA of Nlgn2 KO mice. (A) Photomicrographs show perisomatic VIAAT expression in BA of WT and Nlgn2 KO mice. Scale bar, 2 μ m. (B, C) Mean number per cell perimeter (B) and mean area (C) of perisomatic VIAAT puncta. (D) Photomicrographs show overall localization and expression levels of PV in anterior BA of WT and Nlgn2 KO mice. Scale bar, 20 μ m. (E, F) Total number (E) and mean intensity (F) of PV puncta in analyzed area of BA. $n = 6$ for both genotypes. All bars represent mean + SEM.

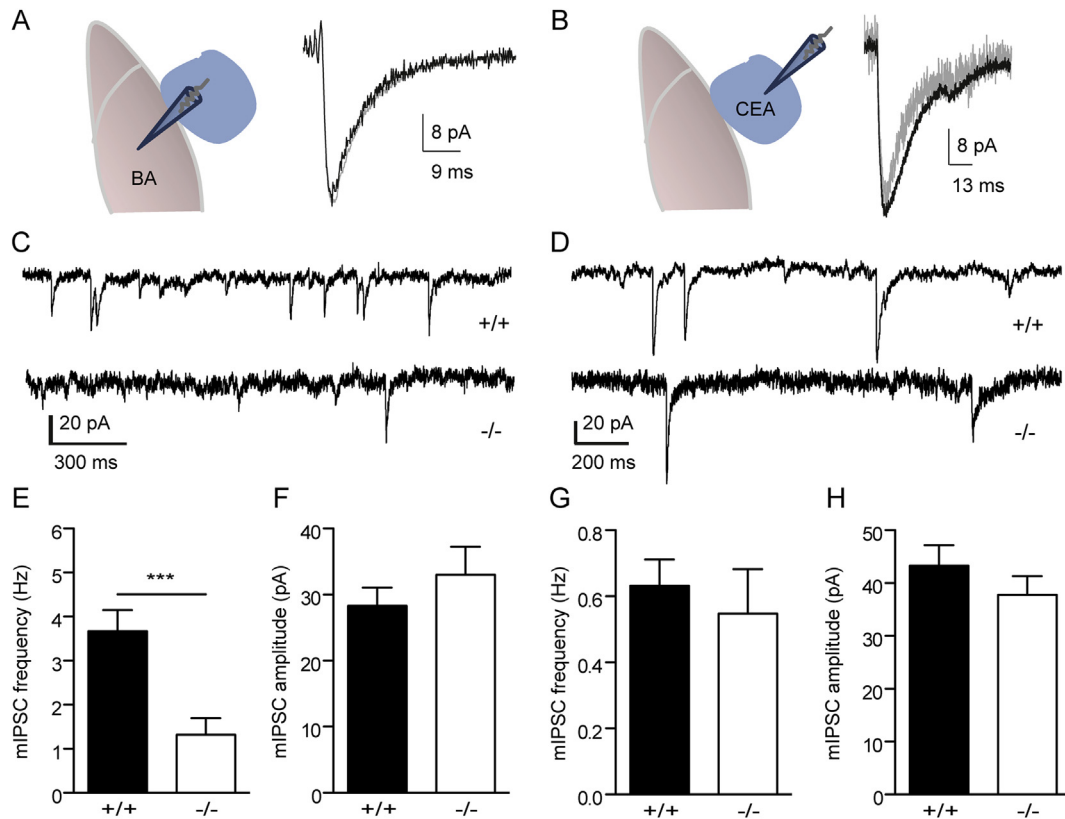


Fig. 6. Effect of Nlgn2 deletion on inhibitory synaptic transmission in BA and CeA. (A, B) Schematic diagram showing the location of recordings and representative miniature IPSCs in BA (A) and CeA (B) of WT (black) and Nlgn2 KO mice (grey). (C, D) Sample traces from BA (C) and CeA (D) of WT and Nlgn2 KO mice. (E, F) Average frequency (E) and amplitude (F) of mIPSCs in BA of WT (black) and Nlgn2 KO mice (white). (G, H) Average frequency (G) and amplitude (H) of mIPSCs in CeA of WT (black) and Nlgn2 KO mice (white). $n = 14$ –15 for both genotypes. Unpaired, two-tailed Student's *t*-test: *** $p < 0.001$. All bars represent mean + SEM.

projection neurons and local inhibitory interneurons (Ehrlich et al., 2009; Sah et al., 2003), each of which play a distinct role in the acquisition and expression of fear- and anxiety-related behavioral outputs (Tye et al., 2011; Wolff et al., 2014). To understand the circuitry underlying the behavioral phenotype in Nlgn2 KO mice, it was therefore essential to investigate the influence of Nlgn2 deletion on distinct amygdala cell types. To dissect the anxiety-induced activation pattern of several types of neurons that have been previously linked to fear behaviors (Wolff et al., 2014), we performed double labeling of cFOS and CaMKII (as a marker for glutamatergic projection neurons), PV, or somatostatin (SOM) in WT and Nlgn2 KO animals that had been exposed to anxiogenic conditions. We quantified both the total number and the cFOS-positive percentage of each type of neuron. We found that Nlgn2 KO mice exhibit enhanced activation of projection neurons in BA (Fig. 7A,E), with no change in the total number of projection neurons (Fig. 7D). In contrast, the total number of PV-positive cells was significantly increased in Nlgn2 KO mice (Fig. 7B,F), without a significant change in the percentage of PV-positive cells that showed cFOS immunoreactivity (Fig. 7G). Nlgn2 deletion did not have an effect on SOM-positive interneurons, as both their total number and their cFOS-positive fraction were unaltered in Nlgn2 KO mice (Fig. 7C,H,I). These data indicate that Nlgn2 deletion impacts specific types of inhibitory synapses in BA in a manner that leads to an increased anxiety phenotype of the KO mice. In addition, the enhanced PV immunoreactivity indicates a perturbed development, maintenance, or homeostasis of this inhibitory neuronal network in Nlgn2 KO mice.

4. Discussion

Using a combination of behavior assessment, quantitative morphological analysis, and electrophysiology, we show here that Nlgn2 deletion in mice leads to alterations in the structure and function of perisomatic inhibitory synapses in the basal amygdala, accompanied by a prominent anxiety phenotype and a corresponding overactivation of projection neurons under anxiogenic conditions. Our findings provide important insights into the molecular mechanisms by which mutations in Nlgn2 may contribute to phenotypes relevant to psychiatric disorders.

Consistent with previous reports on dissociated neuronal cultures and retina (Hoon et al., 2009; Pouloupoulos et al., 2009; Varoqueaux et al., 2004), our data indicate that Nlgn2 in the BA is localized almost exclusively to inhibitory synapses. Moreover, we show that Nlgn2 deletion in the BA leads to a specific loss of perisomatic inhibitory postsynaptic components, but leaves perisomatic inhibitory presynaptic innervation and overall number of inhibitory pre- or postsynapses in the neuropil unaffected, which is in agreement with previous studies on the hippocampus of Nlgn2 KO mice (Jedlicka et al., 2011; Pouloupoulos et al., 2009). This finding is particularly interesting in light of our observation that almost all gephyrin-positive structures in BA contain Nlgn2, indicating that the loss of Nlgn2 at non-perisomatic synapses is compensated by other synaptic adhesion molecules such as β -dystroglycan (Craig and Kang, 2007; Panzanelli et al., 2011). Our data are also consistent with the observation that Nlgn2 deletion in the cerebral cortex specifically affects synaptic connections made by axons of PV-

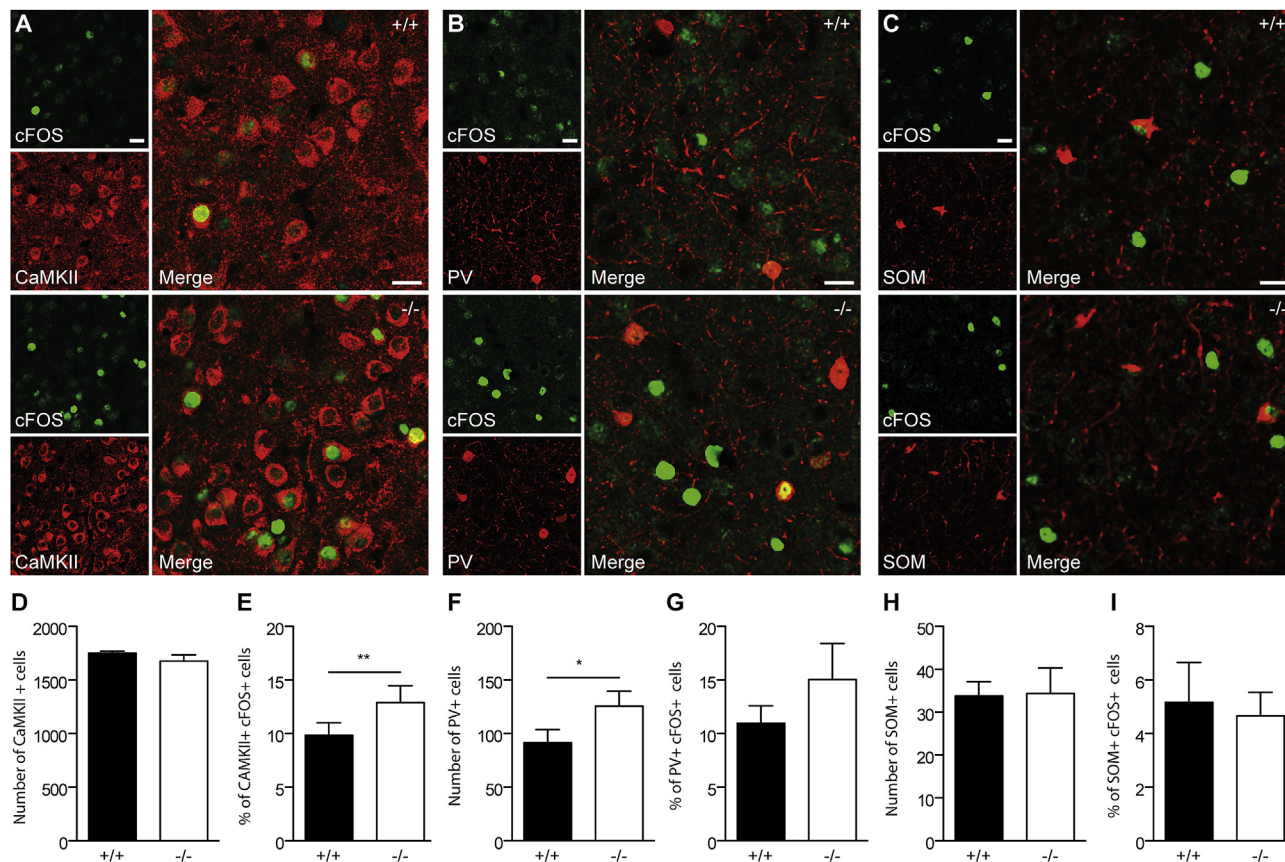


Fig. 7. Effect of Nlgn2 deletion on cellular components of the anxiety circuitry in BA. (A–C) Photomicrographs of anterior BA in WT mice and Nlgn2 KO mice following exposure to stress. The slices were double immunolabeled for cFOS and CaMKII (A), cFOS and PV (B), or cFOS and SOM (C). Scale bar, 50 μ m. (D–I) Number of CaMKII (D), PV (F), and SOM (H) positive cells and percentage of CaMKII (E), PV (G), and SOM (I) positive cells that express cFOS following exposure to stress. For each genotype, $n = 7$ for CaMKII/cFOS analysis, $n = 6$ for analysis of inhibitory markers. Paired Student's *t*-test: * $p < 0.05$, ** $p < 0.01$. All bars represent mean + SEM.

positive interneurons (Gibson et al., 2009), the primary source of perisomatic inhibition in many brain regions, including BA (Muller et al., 2006; Wolff et al., 2014). Interestingly, we observed an increase in the total number of PV-positive interneurons but no change in the number of presynaptic PV-positive terminals, indicating that pruning of the excess inputs may occur during early postnatal development.

In agreement with a key role for Nlgn2 at perisomatic inhibitory synapses in BA, we observed that Nlgn2 deletion results in a pronounced reduction in the frequency, but not the amplitude of mIPSCs in BA. These data may point to a change in presynaptic release probability or, together with our molecular findings, they may indicate that the loss of Nlgn2 reduces the number of functional postsynaptic sites without substantially affecting synaptic transmission at the remaining functional synapses. The mechanism by which deletion of Nlgn2 would affect only a subset of perisomatic synapses is currently unknown, but may potentially be explained by the existence of a molecularly heterogeneous synapse population, in which Nlgn2 is either redundant or not present in some synapses. Interestingly, previous studies have reported differential effects of Nlgn2 deletion on mIPSCs in different brain regions, revealing a pronounced decrease in mIPSC frequency and a lesser decrease in amplitude in area CA1 of hippocampus (Poulopoulos et al., 2009), but a decrease in mIPSC amplitude without accompanying changes in frequency in somatosensory cortex (Gibson et al., 2009) and dentate gyrus (Jedlicka et al., 2011). Together with our current data, these findings again point to a structural and functional heterogeneity of Nlgn2-containing

synapses that warrants further investigation.

The notion that Nlgn2 may function differently at distinct synapses, even on the same neuron, has lately received substantial attention. One recent study showed that deletion of Nlgn3 results in enhanced synaptic transmission at inhibitory connections between cholecystokinin (CCK)-positive interneurons and pyramidal cells in area CA1 of hippocampus, without affecting inhibitory connections formed by PV-positive interneurons onto the same pyramidal cells (Foldy et al., 2013). These and other findings highlight the fact that the effect of Nlgn deletion on circuit function cannot be predicted from studies on dissociated cultures or by inference from other brain regions, but must be investigated in the context of specific behaviorally relevant neural circuits. Accordingly, we report here that despite a near-universal presence of Nlgn2 at inhibitory synapses in BA, only CaMKII-positive glutamatergic projection neurons show differential induction of cFOS in Nlgn2 KO mice under anxiogenic conditions that lead to a prominent anxiety phenotype in these mice. These neurons project to a number of target regions known to mediate anxiety behaviors, including the CEA, hippocampus, bed nucleus of the stria terminalis, and prefrontal cortex (Luthi and Luscher, 2014), and their global activation results in a pronounced anxiety phenotype (Tye et al., 2011). In contrast, the complex inhibitory network of local PV- and SOM-positive interneurons, which play an essential role in regulating neuronal plasticity and learning in the BLA (Wolff et al., 2014), shows no differential cFOS expression under anxiogenic conditions, even though both types of interneurons receive perisomatic innervation from PV-positive terminals (Muller et al.,

2005; Wolff et al., 2014; Woodruff and Sah, 2007). Due to an incompatibility of immunostaining conditions for the Nlgn2 antibody and the PV and SOM antibodies, we cannot rule out the possibility that Nlgn2 may not be expressed in PV- and SOM-positive cells. However, the fact that the vast majority of gephyrin-positive synapses in BA also contain Nlgn2 would argue against this scenario. Alternatively, it is possible that differential compensation by other synaptic adhesion molecules may prevent altered activation of interneurons but not projection neurons, or that under our experimental conditions, acute activation of these interneurons does not play a primary role in the anxiety circuitry. Regardless of the mechanism, our data support a model according to which reduced perisomatic inhibition at connections between PV-positive interneurons and projection neurons in BA of Nlgn2 KO mice results in specific overactivation of these projection neurons under anxiogenic conditions, consistent with the exaggerated behavioral anxiety response. Further studies will be required to further assess the causal role for these connections in the anxiety phenotype, and to identify the molecular mechanisms for the specificity and the relevant downstream circuitry targeted by the glutamatergic BA projections.

Taken together, the findings presented here have important implications for the treatment of anxiety and other comorbid disorders. It has long been known that certain classes of anxiolytic drugs such as benzodiazepines act by enhancing GABAergic synaptic transmission (Macdonald and Barker, 1978), but these drugs act non-specifically at the vast majority of inhibitory synapses in the central nervous system and hence cause a number of undesirable and potentially dangerous side effects. By identifying particular synaptic connections that are especially relevant to the generation of pathological anxiety behaviors, it may be possible to develop improved therapeutic strategies that target these synapses more specifically and are better suited to the treatment of at least a subset of anxiety disorders. Moreover, mutations in Nlgn2 have been linked to schizophrenia (Sun et al., 2011), which shows a high comorbidity with anxiety disorders (Braga et al., 2013). Interestingly, schizophrenia is also associated with deficits in PV-positive interneuron function (Lewis et al., 2012), raising the intriguing possibility that alterations in the function of Nlgn2 may contribute to the comorbid anxiety symptoms in schizophrenia specifically through their effect on perisomatic inhibitory synapses. Further investigation of the precise link between Nlgn2 and behavioral phenotypes related to psychiatric disorders may provide essential insights into underlying molecular mechanisms and potential drug targets for the treatment of these disorders.

Author contributions

O.B., D.K.B., A.L. and N.B. designed the study; O.B. and D.K.B. conducted anxiety and locomotor testing; O.B. conducted immunohistochemistry experiments; P.B. and E.M. conducted electrophysiology experiments; A.L. advised on electrophysiology; H.E. advised on anxiety and locomotor testing; N.B. advised on immunohistochemistry experiments; O.B., D.K.B. and P.B. analyzed data; and O.B. and D.K.B. wrote the manuscript. All authors discussed the results and implications and commented on the manuscript at all stages.

Acknowledgments

This work was supported by the Max Planck Society (N.B., H.E.) and the European Commission (EU-AIMS FP7-115300, N.B., H.E.; Marie Curie IRG, D.K.-B.). O.B. is a student of the Göttingen Graduate School of Neurosciences and Molecular Biosciences (GGNB) and is funded by a PhD fellowship from the Minerva Foundation. D.K.-B.

was supported by Alexander von Humboldt-Foundation. The authors thank F. Benseler, I. Thanhäuser, D. Schwerdtfeger, S. Wenger, A. Ronnenberg, D. Winkler and K. Bylund for valuable advice and excellent technical support, and the MPIEM animal facility for mouse management.

The authors report no biomedical financial interests or potential conflicts of interest.

Appendix A. Supplementary data

Supplementary data related to this article can be found at <http://dx.doi.org/10.1016/j.neuropharm.2015.06.016>.

References

- Blundell, J., Tabuchi, K., Bolliger, M.F., Blaiss, C.A., Brose, N., Liu, X., Sudhof, T.C., Powell, C.M., 2009. Increased anxiety-like behavior in mice lacking the inhibitory synapse cell adhesion molecule neuroligin 2. *Genes Brain Behav.* 8, 114–126.
- Braga, R.J., Reynolds, G.P., Siris, S.G., 2013. Anxiety comorbidity in schizophrenia. *Psychiat. Res.* 210, 1–7.
- Craig, A.M., Kang, Y., 2007. Neurexin-neuroligin signaling in synapse development. *Curr. Opin. Neurobiol.* 17, 43–52.
- Ehrlich, I., Humeau, Y., Grenier, F., Ciochi, S., Herry, C., Luthi, A., 2009. Amygdala inhibitory circuits and the control of fear memory. *Neuron* 62, 757–771.
- Foldy, C., Malenka, R.C., Sudhof, T.C., 2013. Autism-associated neuroligin-3 mutations commonly disrupt tonic endocannabinoid signaling. *Neuron* 78, 498–509.
- Gibson, J.R., Huber, K.M., Sudhof, T.C., 2009. Neuroligin-2 deletion selectively decreases inhibitory synaptic transmission originating from fast-spiking but not from somatostatin-positive interneurons. *J. Neurosci.* 29, 13883–13897.
- Graf, E.R., Zhang, X., Jin, S.X., Linhoff, M.W., Craig, A.M., 2004. Neurexins induce differentiation of GABA and glutamate postsynaptic specializations via neuroligins. *Cell* 119, 1013–1026.
- Hoon, M., Bauer, G., Fritschy, J.M., Moser, T., Falkenburger, B.H., Varoquaux, F., 2009. Neuroligin 2 controls the maturation of GABAergic synapses and information processing in the retina. *J. Neurosci.* 29, 8039–8050.
- Jedlicka, P., Hoon, M., Papadopoulos, T., Vlachos, A., Winkels, R., Pouloupoulos, A., Betz, H., Deller, T., Brose, N., Varoquaux, F., Schwarzscher, S.W., 2011. Increased dentate gyrus excitability in neuroligin-2-deficient mice in vivo. *Cereb. Cortex* 21, 357–367.
- Krueger, D.D., Tuffy, L.P., Papadopoulos, T., Brose, N., 2012. The role of neurexins and neuroligins in the formation, maturation, and function of vertebrate synapses. *Curr. Opin. Neurobiol.* 22, 412–422.
- Lewis, D.A., Curley, A.A., Glausier, J.R., Volk, D.W., 2012. Cortical parvalbumin interneurons and cognitive dysfunction in schizophrenia. *Trends Neurosci.* 35, 57–67.
- Luthi, A., Luscher, C., 2014. Pathological circuit function underlying addiction and anxiety disorders. *Nat. Neurosci.* 17, 1635–1643.
- Macdonald, R., Barker, J.L., 1978. Benzodiazepines specifically modulate GABA-mediated postsynaptic inhibition in cultured mammalian neurones. *Nature* 271, 563–564.
- Muller, J.F., Mascagni, F., McDonald, A.J., 2005. Coupled networks of parvalbumin-immunoreactive interneurons in the rat basolateral amygdala. *J. Neurosci.* 25, 7366–7376.
- Muller, J.F., Mascagni, F., McDonald, A.J., 2006. Pyramidal cells of the rat basolateral amygdala: synaptology and innervation by parvalbumin-immunoreactive interneurons. *J. Comp. Neurol.* 494, 635–650.
- Panzanelli, P., Gunn, B.G., Schlatter, M.C., Benke, D., Tyagarajan, S.K., Scheiffele, P., Belelli, D., Lambert, J.J., Rudolph, U., Fritschy, J.M., 2011. Distinct mechanisms regulate GABA receptor and gephyrin clustering at perisomatic and axo-axonic synapses on CA1 pyramidal cells. *J. Physiol.* 589, 4959–4980.
- Pouloupoulos, A., Aramuni, G., Meyer, G., Soykan, T., Hoon, M., Papadopoulos, T., Zhang, M., Paarmann, I., Fuchs, C., Harvey, K., Jedlicka, P., Schwarzscher, S.W., Betz, H., Harvey, R.J., Brose, N., Zhang, W., Varoquaux, F., 2009. Neuroligin 2 drives postsynaptic assembly at perisomatic inhibitory synapses through gephyrin and collybistin. *Neuron* 63, 628–642.
- Rothwell, P.E., Fuccillo, M.V., Maxeiner, S., Hayton, S.J., Gokce, O., Lim, B.K., Fowler, S.C., Malenka, R.C., Sudhof, T.C., 2014. Autism-associated neuroligin-3 mutations commonly impair striatal circuits to boost repetitive behaviors. *Cell* 158, 198–212.
- Sagar, S.M., Sharp, F.R., Curran, T., 1988. Expression of c-fos protein in brain: metabolic mapping at the cellular level. *Science* 240, 1328–1331.
- Sah, P., Faber, E.S., Lopez De Armentia, M., Power, J., 2003. The amygdaloid complex: anatomy and physiology. *Physiol. Rev.* 83, 803–834.
- Singewald, N., Salchner, P., Sharp, T., 2003. Induction of c-Fos expression in specific areas of the fear circuitry in rat forebrain by anxiogenic drugs. *Biol. Psychiat.* 53, 275–283.
- Soykan, T., Schneeberger, D., Tria, G., Buechner, C., Bader, N., Svergun, D., Tessmer, I., Pouloupoulos, A., Papadopoulos, T., Varoquaux, F., Schindelin, H., Brose, N., 2014. A conformational switch in collybistin determines the differentiation of

- inhibitory postsynapses. *EMBO J.* 33, 2113–2133.
- Spampanato, J., Polepalli, J., Sah, P., 2011. Interneurons in the basolateral amygdala. *Neuropharmacology* 60, 765–773.
- Sudhof, T.C., 2008. Neuroligins and neurexins link synaptic function to cognitive disease. *Nature* 455, 903–911.
- Sun, C., Cheng, M.-C., Qin, R., Liao, D.-L., Chen, T.-T., Koong, F.-J., Chen, G., Chen, C.-H., 2011. Identification and functional characterization of rare mutations of the neuroligin-2 gene (NLGN2) associated with schizophrenia. *Hum. Mol. Genet.* 20, 3042–3051.
- Tye, K.M., Prakash, R., Kim, S.Y., Fenno, L.E., Grosenick, L., Zarabi, H., Thompson, K.R., Gradinaru, V., Ramakrishnan, C., Deisseroth, K., 2011. Amygdala circuitry mediating reversible and bidirectional control of anxiety. *Nature* 471, 358–362.
- Varoqueaux, F., Aramuni, G., Rawson, R.L., Mohrmann, R., Missler, M., Gottmann, K., Zhang, W., Sudhof, T.C., Brose, N., 2006. Neuroligins determine synapse maturation and function. *Neuron* 51, 741–754.
- Varoqueaux, F., Jamain, S., Brose, N., 2004. Neuroligin 2 is exclusively localized to inhibitory synapses. *Eur. J. Cell Biol.* 83, 449–456.
- Wohr, M., Silverman, J.L., Scattoni, M.L., Turner, S.M., Harris, M.J., Saxena, R., Crawley, J.N., 2013. Developmental delays and reduced pup ultrasonic vocalizations but normal sociability in mice lacking the postsynaptic cell adhesion protein neuroligin2. *Behav. Brain Res.* 251, 50–64.
- Wolff, S.B., Grundemann, J., Tovote, P., Krabbe, S., Jacobson, G.A., Müller, C., Herry, C., Ehrlich, I., Friedrich, R.W., Letzkus, J.J., Luthi, A., 2014. Amygdala interneuron subtypes control fear learning through disinhibition. *Nature* 509, 453–458.
- Woodruff, A.R., Sah, P., 2007. Networks of parvalbumin-positive interneurons in the basolateral amygdala. *J. Neurosci.* 27, 553–563.